Composites Science and Technology 94 (2014) 111–116

Contents lists available at ScienceDirect

Composites Science and Technology

journal homepage: www.elsevier.com/locate/compscitech

Facile preparation of superhydrophobic surfaces with enhanced releasing negative air ions by a simple spraying method

Zhaofeng Wu [a], Hua Wang [a], Meng Xue [b], Xingyou Tian [a,*], Xianzhu Ye [a], Haifeng Zhou [a], Zhongyue Cui [a]

[a] Key Laboratory of Materials Physics, Institute of Solid State Physics, Chinese Academy of Sciences, Hefei 230031, PR China
[b] Institute of Environmental Engineering, ETH Zurich, CH-8093 Zurich, Switzerland

ARTICLE INFO

Article history:
Received 17 November 2013
Received in revised form 20 January 2014
Accepted 24 January 2014
Available online 3 February 2014

Keywords:
A. Functional composites
B. Surface treatments
B: Synergism
C: Modelling

ABSTRACT

Superhydrophobic surfaces with micro/nano structures were prepared using the synergistic effect of the hydroxyl-silicone-oil modified microscale tourmaline particles (HTP) and the nanoscale silica (SiO_2) by a simple spraying method. The SiO_2/HTP/Polyurethane (PU) and HTP/PU dispersions were sprayed onto the waterborne polyurethane (WPU) film using a shower nozzle driven by an air compressor. After drying of the spraying film at room temperature, a surface with micro/nano structures was obtained and the micro/nano structures were consisted of the microscale HTP coated by the nanoscale SiO_2. Static water contact angle measurements proved that the rough surfaces were superhydrophobic. Furthermore, their performance of releasing negative air ion was significantly enhanced due to the rough structure. Importantly, this method is simple, low-cost and suitable for the fast and large-scale preparation of superhydrophobic surfaces, which is particularly important for the modification of hydrophilic polymer surfaces.

1. Introduction

Materials with superhydrophobic surfaces have recently received significant attention because of its importance in many biological processes and technological applications, which include self-cleaning surfaces, antifouling or foul-release coatings, stain resistant textiles, non-icing or ice repellant surfaces, etc. [1]. Two descriptions have been proposed for the dependence of the wetting behavior on surface roughness: the Wenzel and Cassie–Baxter models. The Wenzel model [2,3] holds for cases where the liquid remains in contact with the whole solid surface. The enhancement of hydrophobicity is quantitatively described by the Wenzel equation:

$$\cos\theta^{W} = r\cos\theta^{E} \tag{1}$$

where θ^{W} is the observed angle on the rough surface, θ^{E} is the equilibrium contact angle on the flat surface of the same chemical character, and r (with $r \geqslant 1$) is the ratio of the actual surface area to the projected area of the surface. This equation indicates that the surface roughness enhances the hydrophobicity of hydrophobic ones because r is always larger than 1.

The Cassie–Baxter model [4] holds for surfaces with a topography such that water cannot deeply penetrate and wet the whole surface, thus air is trapped into the grooves under the droplet, which is then suspended across the surface protrusions. In such a case, the droplet is in contact with a composite surface (solid and air) and the observed contact angle θ^{CB}, according to the Cassie–Baxter equation, is given by the linear combination:

$$\cos\theta^{CB} = f^{S}\cos\theta^{S} + f^{air}\cos\theta^{air} \tag{2}$$

By considering the air area fraction as $f^{air} = 1 - f^{S}$, $\theta^{air} = 180^{\circ}$, and assuming that the water contact angles of the solid fraction, θ^{S}, corresponds to that of the flat surface, θ^{E}, Eq. (2) can be rewritten as:

$$\cos\theta^{CB} = f^{S}\cos\theta^{E} + (1 - f^{S}) \tag{3}$$

Therefore, in this model, the hydrophobic character of a rough surface is enhanced by the decrease of the solid–liquid contact area [5].

According to the above theories, superhydrophobic surfaces have been prepared by a number of techniques including lithography [6], sol–gel processing [7], electrospinning [8], electrochemical methods [9] chemical vapor deposition [10] and others [1,11]. However, these methods are complex, time-consuming, expensive and not suitable for the fast and large-scale production in current stage. Recently, spray deposition, an alternative low-cost technique to rapidly coat a polymer solution on a variety of substrates to prepare polymer films, has been developed. Karapanagiotis et al. [12] prepared the superhydrophobic films by spraying hydrophilic

* Corresponding author. Tel.: +86 55165591477; fax: +86 55165591434.
E-mail address: xytian@issp.ac.cn (X. Tian).

http://dx.doi.org/10.1016/j.compscitech.2014.01.019
0266-3538/

silica (SiO_2)/poly(methyl methacrylate) (PMMA) suspensions and SiO_2/a commercial poly(alkyl siloxane) on glass surfaces. Bayer et al. [13] reported a superhydrophobic cellulose-based bionanocomposite fabricated by spraying a blend of cellulose nitrate and fluoroacrylic polymer dispersed in modified Pickering emulsions onto aluminum substrates. Zhu et al. [14] reported a superhydrophobic carbon nanotube film fabricated by one-step spray-coating method without any chemical modification on which the wettability can be reversibly switched between superhydrophobic and superhydrophilic by the alternation of UV irradiation and dark storage. Yilgor et al. [15] developed a multi-step spin-coating process that the dispersion of hydrophobic SiO_2 in tetrahydrofuran is coated onto a desired polymer surface to prepare polymer materials with superhydrophobic surfaces. However, the preparation of SiO_2 dispersions used in the coating process requires ultrasonic dispersion for 3 h at room temperature, requiring lots of energy and time. Srinivasan et al. [16] described a similar spraying technique to fabricate various microtextured surfaces from a polymer solution containing a perfluorinated dispersant, with the ability to control the morphology from fibers to beads-on-string and corpuscular structures. The incorporation of the low surface energy 1H, 1H, 2H, 2H-heptadecafluorodecyl polyhedral oligomeric silsesquioxane in the polymer solution confers these microtextured surfaces with significantly enhanced liquid-repellent properties.

In this article, superhydrophobic surfaces with micro/nano structures were prepared using the synergistic effect of the hydroxyl-silicone-oil modified microscale tourmaline particles (HTP) and the nanoscale SiO_2 by a simple spraying method. The SiO_2/HTP/Polyurethane (PU) and HTP/PU dispersions were sprayed onto the waterborne polyurethane (WPU) film to improve its hydrophobic properties. Furthermore, the performance of releasing negative ion was significantly enhanced due to the rough structure.

2. Material and methods

2.1. Materials

TP was purchased from Bao Hua Aion Powder Co., Ltd., Shenzhen, China. Hydrophobic SiO_2 HDK H2000 (H2K) was kindly provided by Wacker Chemie, Munich, Germany. Polytetramethylene glycol (PTMG, Mn = 2000), polycaprolactone glycol (PCL, Mn = 2000) and 4, 4-diphenyl methane diisocyanate (MDI) were supplied by An Li Artificial Leather Co., Ltd., Hefei, China. Petroleum ether, butanediol (BD), acetone, triethylamine (TEA), and butanediol (BD) and N, N-dimethylformamide (DMF) were purchased from Sinopharm Chemical Reagent Co., Ltd., Beijing, China. Hydroxyl silicone oil (HSO, C_{OH} = 280 mg KOH/g) was obtained from Foshan Vago Organic Silicon Co., Ltd., Guangzhou, China. Dimethylol propionic acid (DMPA) was obtained from Aladdin Reagent, Shanghai, China.

2.2. Modification of TP by grafting HSO

HSO and TP were heated at 100 °C under reduced pressure (5 Torr) for 6 h. Then, HSO and TP with the mass ratio of 1 to 1 were put into an autoclave and mixed by stirring. After mixing, they were sealed in the autoclave under nitrogen atmosphere and heated at 140 °C for 12 h. The treated TP was repeatedly washed using petroleum ether by vacuum filtration. The filtrate cake was placed in a vacuum oven at 90 °C for 12 h. At last, the dried cake was ground and sieved with a 200 mesh sieve to obtain the HSO-modified TP, which is designated as the HTP.

2.3. Preparation of WPU emulsions and WPU films

12.5 g of MDI, 20.0 g of PTMG, 20.0 g of PCL and 2.68 g of DMPA were put into a 500 ml three-necked flask equipped with a condenser tube, dropping funnel, and mechanical stirrer to react at 75 °C for about 3 h under nitrogen atmosphere. Then the NCO-terminated prepolymer was obtained. According to the NCO value determined by the standard dibutylamine titration method (HG/T 2409-92), a stoichiometric amount of BD dissolved in 40 ml acetone was added dropwise to extend the chain at 60 °C until the theoretical NCO content was reached. After that, the reaction mixture was cooled to 40 °C, and 2.1 g of TEA was added to neutralize the carboxylic groups of DMPA. After 30 min neutralization, distilled water was added to the mixture with vigorous stirring to obtain the WPU emulsion with the solid content of about 30 wt%. At last, the WPU emulsion was cast glass substrates and dried at 80 °C for 12 h to obtain the WPU films.

2.4. Preparation of HTP/PU and SiO_2/HTP/PU dispersions

A 500 ml three-necked flask equipped with a condenser tube, dropping funnel, and mechanical stirrer was charged with 10.0 g of MDI, 20.0 g of PTMG, 20.0 g of PCL and HTP at 75 °C. The mixture in the three-necked flask reacted at 75 °C for about 3 h with stirring to obtain the prepolymer. The temperature was then reduced to 60 °C, and a stoichiometric amount of BD dissolved in 60 ml DMF was added dropwise to extend the chain until the theoretical NCO content was reached. DMF was added in the process of expanding chain in order to reduce the viscosity of reaction system. At last, the 5 wt% HTP/PU dispersion with a solid content of about 30% was obtained, which was diluted in DMF to obtain the diluted HTP/PU dispersion with a solid content of about 10%. The 5 wt% TP/PU, 2 wt% SiO_2/5 wt% TP/PU and 2 wt% SiO_2/5 wt% HTP/PU dispersions were also prepared in the similar way.

2.5. Sample preparation by spraying

The spraying equipment is a shower nozzle driven by an air compressor, which is similar with Srinivasan's report. [16] The

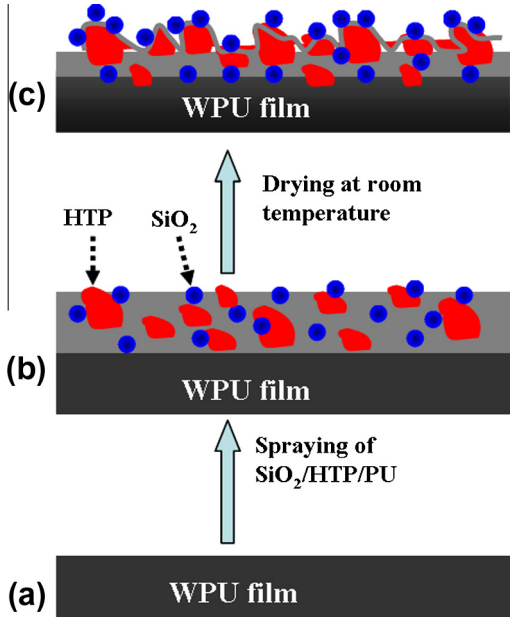

Fig. 1. Schematic of the preparation of superhydrophobic surfaces. (a) WPU film, (b) Spraying of SiO_2/HTP/PU dispersion, and (c) surfaces with micro/nano structures after drying.

process of sample preparation by spraying is illustrated in Fig. 1, which is similar with Yilgor's report [15]. As shown in Fig. 1b, the diluted HTP/PU and SiO_2/HTP/PU dispersions with a solid content of about 10% were sprayed on the WPU films. The spraying films were slowly dried at room temperature. In the process of drying, the surface layer of WPU films were dissolved by DMF, which allowed the penetration of HTP and SiO_2 into the surface layer of WPU films (Fig. 1c). Thus, there was a strong adhesive between the WPU films and the spraying layer. After drying, HTP and SiO_2 were partly protruded out, which formed the micro/nano structures (Fig. 1c).

2.6. Characterization

The sample and KBr were pressed to form a tablet and their spectra were recorded on a Nicolet Nexus Fourier transform infrared (FTIR) spectrometer. Thermal gravimetric analysis (TGA) was carried out using a Q5000 IR thermal gravimetric analyzer with a heating rate of 10 °C/min under nitrogen condition. Water contact angles were measured using a FTA-1000B contact angle goniometer (First Ten Angstrom, USA), and the values reported were the average of three drops per sample at different locations. The morphology of samples was observed under a Sirion-200 SEM (FEI, America) with an accelerating voltage of 10 kV. The concentration of negative air ions emitted from the samples prepared by the spraying method and the samples prepared by the casting method were determined using an air ion detector (model COM-3010 PRO, made in Japan). The concentration of negative air ions reported is an average value of five measurements.

3. Results and discussion

3.1. Modification of TP by grafting HSO

FTIR spectra were used to characterize the HTP as shown in Fig. 2. The raw TP exhibited absorption bands at 3560 cm^{-1} (–OH) and 985 cm^{-1} (Si–O). The FTIR spectrum of HSO showed a strong Si–O–Si stretching absorption at 1033 and 1092 cm^{-1}, which was characteristic of a siloxane backbone. [17,18] The CH_3 bending and rocking peaks were observed at 1262 and 800 cm^{-1}. [18] It can be clearly seen that the FTIR spectrum of the HTP reveals new absorptions compared with the raw TP. The new absorptions at 1262 cm^{-1} (Si–CH_3), 1098, 1021 cm^{-1} (Si–O–Si), and 800 cm^{-1} (CH_3–Si) for the HTP were ascribed to the HSO groups, [17] indicating that the HSO groups were successfully grafted onto the TP.

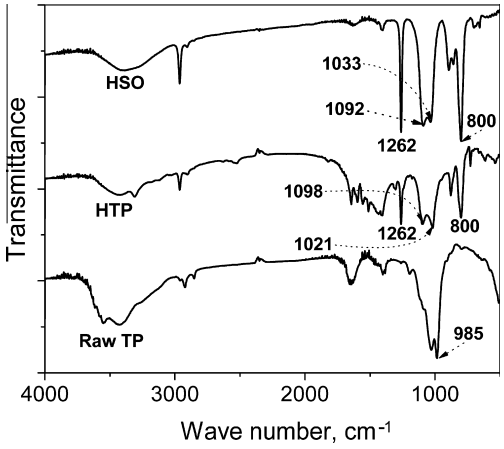

Fig. 2. FTIR spectra of HSO, raw TP and HTP.

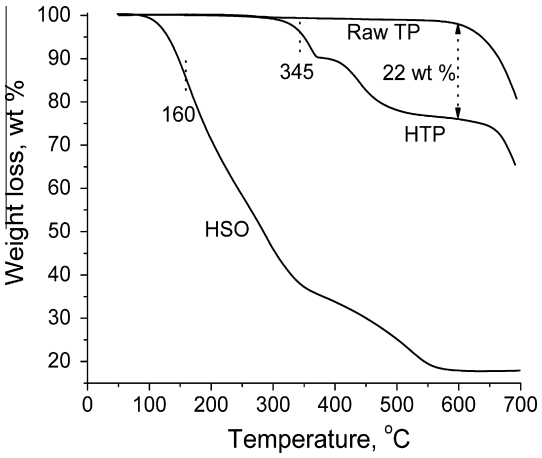

Fig. 3. TGA curves of HSO, raw TP and HTP.

TGA was also used to confirm the grafting of HSO on the surface of the TP. Fig. 3 shows the TGA curves of the HSO, raw TP and HTP. As shown in Fig. 3, the HSO exhibits a rapid weight loss starting at 160 °C, and has nearly 60 wt% weight loss between 150 and 400 °C, compared with the good thermal stability of the raw TP below 500 °C. For the HTP, the weight loss due to the decomposition of organic species is observed in the range of 300–600 °C, which suggests that the HSO has been chemically grafted onto the surfaces of the TP and the grafting improves significantly the thermal stability of the HSO on the surfaces of the TP. The mass percentage of the grafted HSO onto the HTP was estimated to be 22 wt% according to the residues of the raw TP and the HTP at 600 °C in Fig. 3.

3.2. Surface structure and morphology

To investigate the surface morphology of the samples prepared by the spraying method and their effect on the hydrophobic behavior, we performed SEM observations on the sample surfaces. As shown by SEM images with different magnifications in Fig. 4, the microscale rough structures were formed on the surfaces by spraying the HTP/PU dispersion, which was somewhat similar with the surface morphologies of cellulose-based composite films and the composite films containing hydrophilic SiO_2 prepared by the spraying method. [12,13] The rough structures on the surfaces were mainly consisted of the HTP with diameters of 1–20 μm (Fig. 4a and b). It is worth noting that the surfaces of the HTP are covered by a layer of PU film with many microporous (Fig. 4c and d), which indicates that the HTP has a good compatibility with the PU matrix. The good compatibility contributes to the long-term stable adhesion of the HTP on the surfaces, which is helpful for keeping the stability and persistence of the rough surface. These rough structures will play an important role in the enhancement of hydrophobic behaviors.

For the surfaces by spraying the SiO_2/HTP/PU dispersion, a similar rough structure was formed as shown by SEM images with different magnifications in Fig. 5. As shown in Fig. 5a and b, the microscale rough structures were formed on the surfaces after spraying the SiO_2/HTP/PU dispersion and the rough structures were also mainly consisted of the TP with diameters of 1–20 μm. Although the surfaces of the HTP were also covered by a layer of PU film with microporous (Fig. 4c and d), the number of the microporous decreased significantly and the PU film was covered by a layer of SiO_2 particles. TP is a natural silicate mineral with the strong polarity exhibiting both pyroelectric and piezoelectric properties. [19–21] Electric fields on the order of 10^5–10^7 V/m exist on the surface of the micrometer-sized TP [22], even 10^7–10^9 V/m for

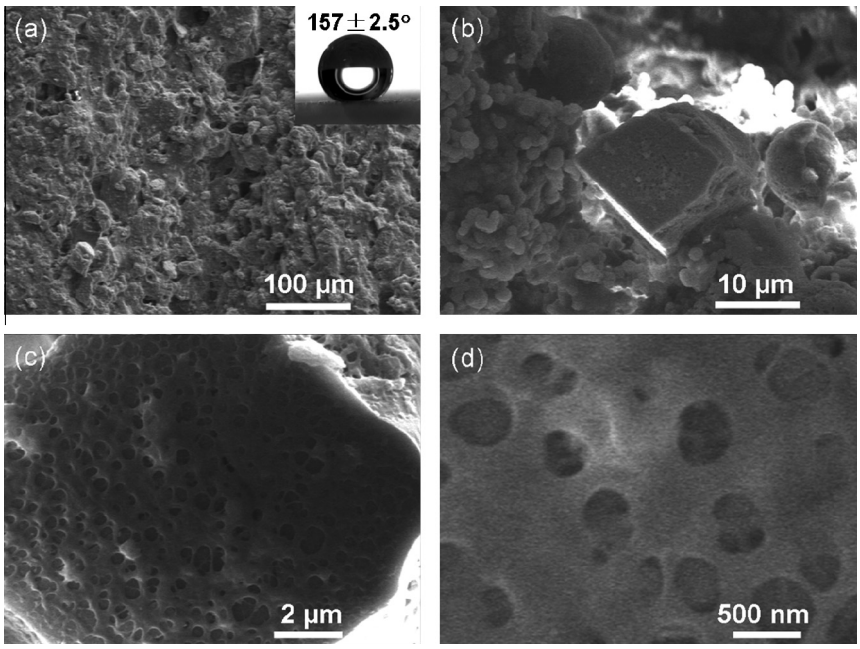

Fig. 4. (a)–(d) SEM images with different magnifications of surfaces by spraying the HTP/PU dispersion. The inset is the image of water drop and the water contact angle.

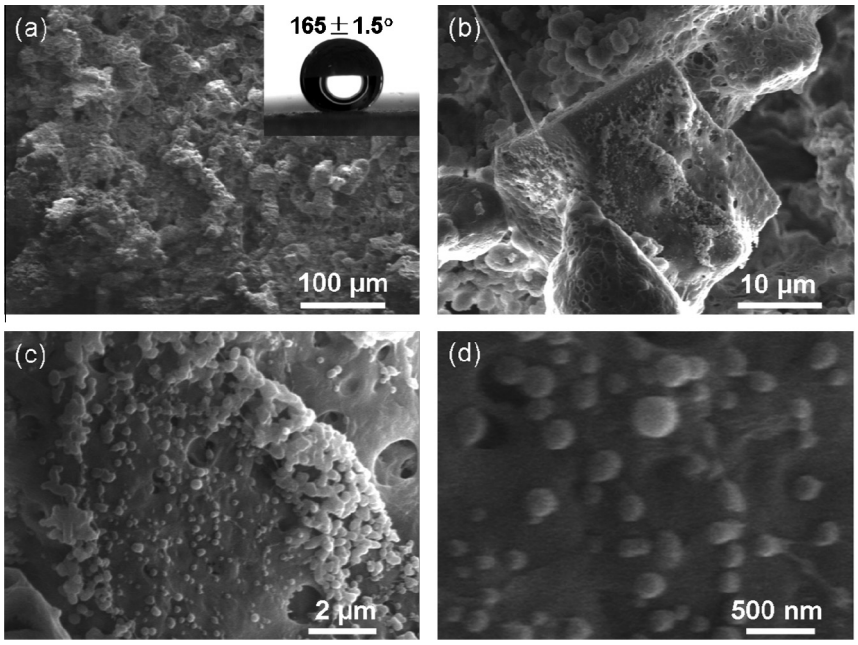

Fig. 5. (a)–(d) SEM images with different magnifications of surfaces by spraying the SiO_2/HTP/PU dispersion. The inset is the image of water drop and the water contact angle.

the nanometer-sized TP [23,24]. Therefore, the phenomenon that TP is covered by a layer of SiO_2 particles should be attributed to the strong polarity and electric fields of the TP, that is, the microscale TP and the nanoscale SiO_2 play the synergistic role in the formation of surfaces with micro/nano structures.

In order to better illustrate the effect of the spraying method on surface morphology, the surface morphology of the HTP/PU film prepared by casting the HTP/PU dispersion with a solid content of about 10% was also investigated in Fig. 6. Compared with the rough surfaces prepared by the spraying method (Fig. 4), the surfaces prepared by the casting method were nearly smooth (Fig. 6a and b). As shown in Fig. 6, the HTP is almost immersed in the PU matrix and only a part surface of the HTP was above the surface of the PU matrix. The sharp contrast indicated that the spraying method could be used to effectively prepare the surface with rough structures, which play an important role in the enhancement of liquid-repellent properties.

3.3. Enhanced liquid-repellent properties

The enhanced liquid-repellent properties of the surfaces prepared by the spraying method were also confirmed by the liquid droplet tests in Fig. 7. As shown in Fig. 7, all water, red ink and fluid wax droplets with the size of 3–5 mm on the surfaces prepared by

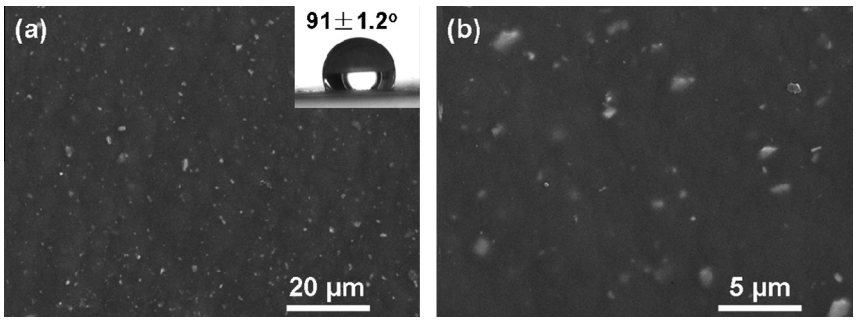

Fig. 6. (a) and (b) SEM images of HTP/PU film prepared by the casting method. The inset is the image of water drop and the water contact angle.

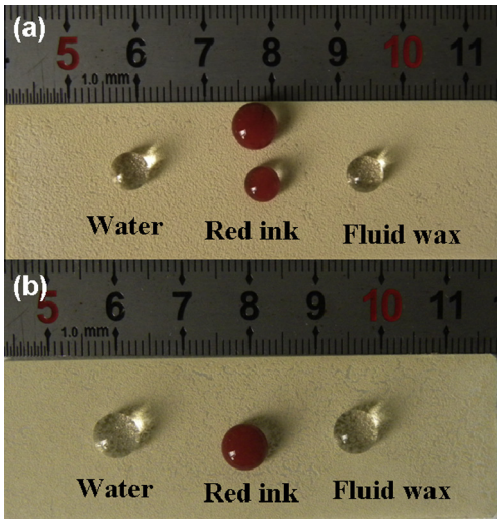

Fig. 7. Images of liquid droplets on the rough surfaces prepared by spraying the (a) HTP/PU dispersion, and (b) SiO_2/HTP/PU dispersion.

spraying the PU/TP (Fig. 7a) and the surfaces prepared by spraying the SiO_2/PU/TP (Fig. 7b) did not spread, keeping the liquid spheres very well, which indicated that the surfaces prepared by the spraying method showed the good hydrophobic and oleophobic performances. The ultimate test to prove the formation of superhydrophobic surfaces was the static water contact angle measurements. As shown by the inset in Fig. 6, the static water contact angle of the samples prepared by casting the HTP/PU dispersion reached about 91°. While the static water contact angles of the samples prepared by spraying the HTP/PU and SiO_2/HTP/PU dispersion reached about 157° and 165° (the insets in Fig. 4 and Fig. 5), respectively. It also can be seen that the contact angle of the sample prepared by spraying SiO_2/HTP/PU is higher than that of the sample prepared by spraying HTP/PU due to the addition of hydrophobic SiO_2. The enhanced hydrophobic properties should be attributed to the micro/nano structures constructed by the synergistic effect of the microscale HTP and the nanoscale SiO_2.

Furthermore, in order to illustrate the effect of the modification of TP on liquid-repellent properties, the surface morphology and the water contact angles of the TP/PU and SiO_2/TP/PU films prepared by the spraying method were also investigated in Fig. 8. Although their surface morphology (Fig. 8) was similar with that of the films with the HTP (Figs. 4a and 5a), the static water contact angles reached only 123° and 145° for the TP/PU film and the SiO_2/TP/PU film, respectively. The fact that the water-repellent properties of the films with the HTP were better than the films with the raw TP indicated that both the modification of TP by grafting HSO and the rough structures contributed to the enhanced water-repellent properties. It was worth noting that the addition of the hydrophobic SiO_2 contributed more to the water-repellent properties of the TP/PU film than that of the HTP/PU film, which also illustrated the importance of the modification of TP.

3.4. Enhanced performance of releasing negative ions

It is well known that the TP maintains a pair of electrodes with no supply of external electric energy, which can be recognized as permanent electrodes that can generate negative air ions [23,25]. Biological functions of the person under the influence of negative ions is improved, such as sleep-stimulation, good mood, activation of body cells, acceleration of metabolism, blood circulation and fatigue recovery [26–29]. The average concentration of negative air ions emitted from the samples prepared by casting the HTP/PU dispersion reached 1065 particles/cubic centimeter. Compared with the samples prepared by the casting method, the average concentrations of negative air ions emitted from the samples prepared by spraying the HTP/PU dispersion and SiO_2/HTP/PU dispersion were increased by 87.3% and 85.7%, respectively, reaching 1995 and 1978 particles/cubic centimeter. It can be seen

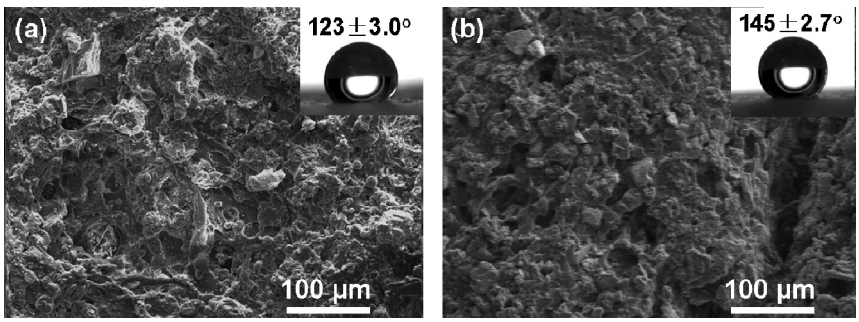

Fig. 8. SEM images of surfaces prepared by spraying the TP/PU (a) and SiO_2/TP/PU (b) dispersions. The insets are the images of water drops and the water contact angles.

that the addition of SiO_2 has almost no effect on the average concentration of negative air ions and the performance of releasing negative ions of the sample surfaces prepared by the spraying method is enhanced obviously. According to the rough structures shown in Figs. 4 and 5, the enhanced performance of releasing negative air ions should be attributed to the special rough structure, which allows the more surfaces of the HTP to contact with air. In addition, aside from the spontaneous electric field and releasing negative air ions, other salient features of the TP include the capacity to shield electric field, self-radiating far infrared ray, as well as antibacterial activity [21,30,31]. Therefore, the addition of the TP will endow the composite films with more functions. The enhanced performance of releasing negative ions, liquid-repellent properties and other functions introduced by the TP will greatly improve the performance/price ratio and market competitiveness, expanding the application fields of the products.

4. Conclusion

Superhydrophobic surfaces with micro/nano structures were successfully prepared using the synergistic effect of the micronscale HTP and the nanoscale SiO_2 by a simple spraying method. After spraying the SiO_2/HTP/PU and HTP/PU dispersions onto the WPU films, the microscale HTP was coated by the nanoscale SiO_2, forming the superhydrophobic surfaces with micro/nano structures. Furthermore, the performance of releasing negative air ions was significantly enhanced because the more surfaces of the HTP were exposed to air due to the rough structure. The enhanced performance of releasing negative ions, liquid-repellent properties and other functions introduced by TP will greatly improve the performance/price ratio and market competitiveness, expanding application fields of the composite products. In addition, this simple and low-cost method is not only suitable for the fast and large-scale preparation of superhydrophobic surfaces, but also provides a new potential route for the preparation of multifunctional superhydrophobic composite films using the synergistic effect of the microscale TP and the nanoscale particles, such as Fe_3O_4, TiO_2, and gold nanoparticles.

Acknowledgment

The authors are grateful to the supports of National Natural Science Foundation of China (No. 51103160).

References

[1] Roach P, Shirtcliffe NJ, Newton MI. Progess in superhydrophobic surface development. Soft Matter 2008;4(2):224–40.
[2] Wenzel RN. Resistance of solid surfaces to wetting by water. Ind Eng Chem 1936;28:988–94.
[3] Wenzel RN. Surface roughness and contact angle. J Phys Colloid Chem 1949;53:1466–7.
[4] Cassie ABD, Baxter S. Wettability of porous surfaces. Trans Faraday Soc 1944;40:546–50.
[5] Mundo RD, Palumbo F, d'Agostino R. Nanotexturing of polystyrene surface in fluorocarbon plasmas: from sticky to slippery superhydrophobic. Langmuir 2008;24(9):5044–51.
[6] Shiu JY, Kuo CW, Chen P, Mou CY. Fabrication of tunable superhydrophobic surfaces by nanosphere lithography. Chem Mater 2004;16(4):561–4.
[7] Shirtcliffe NJ, McHale G, Newton MI, Perry CC. Intrinsically superhydrophobic organosilica sol–gel foams. Langmuir 2003;19(14):5626–31.
[8] Ma M, Hill RM, Lowery JL, Fridrikh SV, Rutledge GC. Electrospun poly(styrene-block-dimethylsiloxane) block copolymer fibers exhibiting superhydrophobic. Langmuir 2005;21(12):5549–54.
[9] Shi F, Wang ZQ, Zhang X. Combining a layer-by-layer assembling technique with electrochemical deposition of gold aggregates to mimic the legs of water striders. Adv Mater 2005;17(8):1005–9.
[10] Lau KKS, Bico J, Teo KBK, Chhowalla M, Amaratunga GAJ, Milne WI, et al. Superhydrophobic carbon nanotube forests. Nano Lett 2003;3(12):1701–5.
[11] Shirtcliffe NJ, McHale G, Atherton S, Newton MI. Adv Colloids Interface Sci 2010;161:124–38.
[12] Manoudis PN, Karapanagiotis I, Tsakalof A, Zuburtikudis I, Panayiotou C. Superhydrophobic composite films produced on various substrates. Langmuir 2008;24(19):11225–32.
[13] Bayer IS, Steele A, Martorana PJ, Loth E, Miller L. Superhydrophobic cellulose-based bionanocomposite films from Pickering emulsions. Appl Phys Lett 2009;94(16):163902–5.
[14] Yang J, Zhang Z, Men X, Xu X, Zhu X. Reversible superhydrophobicity to superhydrophilicity switching of a carbon nanotube film via alternation of UV irradiation and dark storage. Langmuir 2010;26(12):10198–202.
[15] Yilgor I, Bilgin S, Isik M, Yilgor E. Facile preparation of superhydrophobic polymer surfaces. Polymer 2012;53(6):1180–8.
[16] Srinivasan S, Chhatre SS, Mabry JM, Cohen RE, McKinley GH. Solution spraying of poly(methyl methacrylate) blends to fabricate microtextured, superoleophobic surfaces. Polymer 2011;52(14):3209–18.
[17] Bai CY, Zhang XY, Dai JB, Wang JH. Synthesis of UV crosslinkable waterborne siloxane-polyurethane dispersion PDMS-PEDA-PU and the properties of the films. J Coat Technol Res 2008;5(2):251–7.
[18] Wang LF, Ji Q, Glass TE, Ward TC, McGrath JE, Muggli M, et al. Synthesis and characterization of organosiloxane modified segmented polyether polyurethanes. Polymer 2000;41(13):5083–93.
[19] Gavrilova ND, Drozhdin SN, Novik VK, Maksimov EG. Relationship between the pyroelectric coefficient and the lattice-dynamics of the pyroelectrics. Solid State Commun 1983;48(2):129–33.
[20] Gavrilova ND, Maksimov EG, Novik VK, Drozhdin SN. The low-temperature behavior of the pyroelectric coefficient. Ferroelectrics 1989;100:223–40.
[21] Wu Z, Wang H, Zheng K, Xue M, Cui P, Tian X. Incorporating strong polarity minerals of tourmaline with carbon nanotubes to improve the electrical and electromagnetic interference shielding properties. J Phys Chem C 2012;116(23):12814–8.
[22] Yeredla RR, Xu HF. Incorporating strong polarity minerals of tourmaline with semiconductor titania to improve the photosplitting of water. J Phys Chem C 2008;112(2):532–9.
[23] Nakamura T, Kubo T. Tourmaline group crystals reaction with water. Ferroelectrics 1992;137(1–4):13–31.
[24] Lameiras FS, Nunes EHM, Marialeal J. Backgrounds for the industrial use of black tourmaline based on its crystal structure characteristics. Ferroelectrics 2008;377:107–19.
[25] Kubo T. Interface activity of water given rise by tourmaline. Solid State Phys 1989;24(12):303–13.
[26] Yoshinori K, Hikohiro S. Tourmaline composite grains and apparatus using them. US Patent, 6034013; 2000.
[27] Tyushi T, Ryushi T, Kita I, Sakurai T, Yasumatsu M, Isokawa M, et al. The effect of exposure to negative air ions on the recovery of physiological responses after moderate endurance exercise. Int J Biometeorol 1998;41(3):132–6.
[28] Lin Z. The effect of air ions on hygiene. Ecol Sci 1999;18(2):87–90.
[29] Nakane H. Effect of negative air ions on computer operation, anxiety and salivary chromogranin A – like immunoreactivity. Int J Psychophysiol 2002;46(1):85–9.
[30] Ruan D, Zhang LN, Zhang ZJ, Xia XM. Structure and properties of regenerated cellulose/tourmaline nanocrystal composite films. J Polym Sci Pol Phys 2004;42(3):367–73.
[31] Liang JS, Meng JP, Liang GC, Feng YW, Ding Y. Preparation and photocatalytic activity of composite films containing clustered TiO_2 particles and mineral tourmaline powders. T Nonferr Metal Soc 2006;16:s542–6.